

This document is confidential and is proprietary to the American Chemical Society and its authors. Do not copy or disclose without written permission. If you have received this item in error, notify the sender and delete all copies.

Porous Tin-Organic Frameworks as Selective Epimerization Catalysts in Aqueous Solutions

Journal:	<i>ACS Catalysis</i>
Manuscript ID	cs-2017-00806e.R1
Manuscript Type:	Article
Date Submitted by the Author:	n/a
Complete List of Authors:	Delidovich, Irina; RWTH Aachen University, Institut für Technische und Makromolekulare Chemie Hoffmann, Andreas; RWTH Aachen University, Institut für Technische und Makromolekulare Chemie Willms, Andrea; RWTH Aachen University, Institut für Technische und Makromolekulare Chemie Rose, Marcus; RWTH Aachen University, Institut für Technische und Anorganische Chemie

SCHOLARONE™
Manuscripts

This document is the Accepted Manuscript version of a Published Work that appeared in final form in ACS Catalysis copyright © 2017 American Chemical Society after peer review and technical editing by the publisher. To access the final edited and published work see <https://doi.org/10.1021/acscatal.7b00806>.

Porous Tin-Organic Frameworks as Selective Epimerization Catalysts in Aqueous Solutions

Irina Delidovich, Andreas Hoffmann, Andrea Willms, Marcus Rose*

Institut für Technische und Makromolekulare Chemie, RWTH Aachen University, Worringerweg 2, 52074 Aachen, Germany.

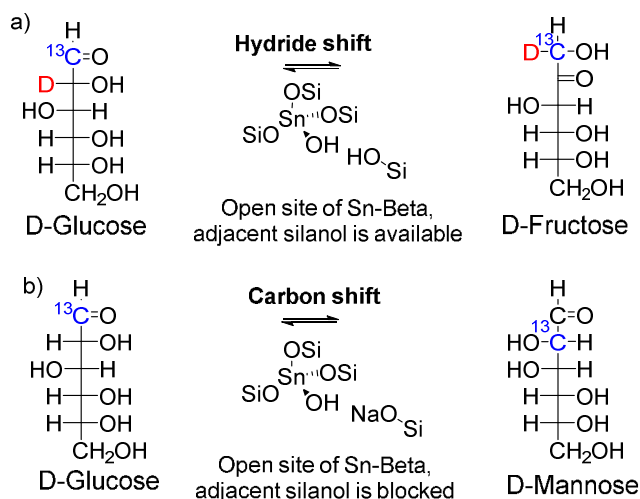
ABSTRACT: Epimerization of sugars is a carbon-efficient route not only to produce rare carbohydrates but also to extend the product scope for chemical production in future biorefineries. Industrially available catalysts for the epimerization are limited mainly to soluble Mo(VI) species as well as substrate-specific epimerases. Here we report a highly active and selective tin-organic frameworks (Sn-OF) as solid catalysts for the epimerization of aldoses at the C-2 position, such as the conversion of glucose to mannose. The reaction proceeds via a carbon skeleton rearrangement, i.e., through breaking of a C-2/C-3 carbon bond and formation of a C-1/C-3 bond. Partially hydrolyzed $\text{Ph}_3\text{Sn-OH}$ sites were found to be the catalytically active centers. Our results suggest that the high catalytic activity of Sn-OFs for the epimerization is determined by (1) Lewis acidity of tin; (2) free Sn-OH groups; and (3) the high hydrophobicity of organic linkers applied in the aqueous solutions.

KEYWORDS: Epimerization, Isomerization, Saccharides, Aldoses, Tin catalyst, Porous organic framework, Aqueous solution

1. INTRODUCTION

Monosaccharides are of great importance in numerous technological sectors, including food industry, pharmaceutical production as well as the synthesis of fine chemicals.¹ Moreover, recent developments in the field of biomass valorization enabled efficient chemical transformations of carbohydrates as a key factor for the production of bio-based fuels and commodity chemicals.² Though many saccharides are highly available in nature, the amount of abundant monosaccharides is limited to seven, namely D-glucose, D-fructose, D-ribose, D-galactose, D-xylose, L-arabinose, and D-mannose. The portfolio of available carbohydrates can be significantly extended by isomerizations as carbon-efficient reactions. Therefore, recent research efforts have been focused on the development of catalysts for the selective isomerization.³ Lately, especially water-tolerant Lewis acidic catalysts attracted great attention.⁴ Among the tested Lewis acids, Sn-Beta zeolite exhibits the highest activity for the isomerization due to optimal structure of the catalyst in terms of high dispersion of the active sites: Tin ions are embedded into a hydrophobic matrix of silicalite which protects Sn^{4+} from hydrolysis in bulk water.⁴⁻⁷ Sn-Beta demonstrated a high selectivity for the isomerization of aldoses into corresponding ketoses, e.g., the transformation of glucose into fructose. Detailed investigations of the reaction mechanism suggested that the isomerization takes place at the open sites, i.e., partially hydrolyzed sites, of Sn-Beta zeolites (Scheme 1a).⁸⁻¹⁰ It was shown that the reaction proceeds via a hydride shift from the C-2 to the C-1 atom of glucose yielding fructose as ketose isomer.¹¹ Importantly, both the Sn atom and the adjacent

silanol group participate in the transition state, as supported by computational methods¹²⁻¹³ and experimental evidences.⁹ Interestingly, Rai et al. performed a computational study of Sn^{4+} as a sole active site of Sn-Beta, i.e. considering an adjacent silanol as a spectator, and predicted a different reaction mechanism (Scheme 1b).¹² According to their calculations, epimerization of an aldose via the 'Bilik mechanism' is energetically preferable in this case. The Bilik reaction^{3, 14-15} is an epimerization accompanied by rearrangement of a carbon skeleton. It involves a bond breaking between C-2 and C-3 carbon atoms of a substrate and the formation of a new bond between C-1 and C-3 atoms (Scheme 1b). Bermejo-Deval et al. proved experimentally the different mechanism in case adjacent silanol groups are not available.⁹ They performed a post-synthetic ion exchange of protons with Na^+ cations to obtain a material which does not possess free OH-groups next to Sn^{4+} active sites. Remarkably, the Na-exchanged Sn-Beta indeed demonstrated high selectivity for epimerization of glucose into mannose via the 'Bilik mechanism' (Scheme 1b). However, this material appeared to be unstable under the reaction conditions due to rapid leaching of Na^+ into the solution. Consequently, the initial selectivity for fructose was quickly restored in the course of the experiment.⁹ More recently, Brand et al. reported on molecular complexes of tin (tin silsesquioxanes) for the carbon shift also proving that the absence of an adjacent silanol group promotes the selective epimerization of aldoses.¹⁶⁻¹⁷ Gunther et al. demonstrated that a combination of Sn-Beta with soluble borate salts selectively catalyzes the epimerization of aldoses, induced by an in-situ formation of saccharide-borate complexes.¹⁸ However, this approach is hardly applicable in industry



Scheme 1. Depending on the active sites of Sn-Beta zeolite two different reaction routes of glucose are known: (a) the isomerization in the presence of adjacent silanol groups and (b) the epimerization induced by isolated stannanol groups.^{9,12}

due to cumbersome separation of the saccharides and borates.¹⁹ To our knowledge, no solid Sn-containing Lewis acidic catalyst has been reported for the selective epimerization of aldoses so far, though heterogeneous catalysis enables an easy catalyst separation and recycling. In general, the number of selective catalysts for epimerization is very limited. Thus, in addition to the aforementioned examples, only Mo(VI)-based catalysts exhibit high selectivity for the epimerization,²⁰ though most of the reported molybdenum catalysts are soluble¹⁵ or undergo leaching of active species under reaction conditions.²¹ Moreover, the majority of epimerases is efficient on saccharides substituted with phosphate or nucleotide groups, but not on free, non-activated carbohydrates.²² Consequently, elaboration of a solid catalyst for epimerization is of great advantage for the synthesis of rare saccharides as well as to widen the scope in the production of novel biogenic platform chemicals.

Herein we report the application of porous tin-organic frameworks (Sn-OF) as solid catalysts that are able to selectively catalyze the epimerization of monosaccharides. These hydrophobic materials exhibit a superposition of partially hydrolyzed tin Lewis acidic centers that are covalently connected by organic aromatic linkers. The synthesis and characterization of the Sn-OF materials was reported initially by Fritsch et al. using a 4,4'-dibromobiphenyl building block.²³ The materials exhibit a high thermal and hydrolytic stability due to covalent bonds between Sn and the organic linker. The application of Sn-OFs as solid catalysts with Lewis acidic centers was so far only reported twice: the cyanosilylation of benzaldehyde²³ and the esterification of oleic acid with glycerol.²⁴ Based on that, we synthesized the Sn-OFs containing 4,4'-dibromobiphenyl (Sn-OF-1) as well as a new one based on 1,3,5-tris-(4-bromophenyl)-benzene (Sn-OF-2) and applied them successfully in the isomerization of

aldoses, namely for the epimeric pairs glucose-mannose, ribose-arabinose, and xylose-lyxose.

2. EXPERIMENTAL SECTION

2.1. Preparation of Catalysts

Syntheses of Sn-OFs were performed under argon atmosphere using Schlenk techniques. Sn-OF-1 was prepared according to the protocol published by Fritsch et al.²³ 4,4'-dibromobiphenyl (3.12 g, 10 mmol) was dissolved in 200 mL of dry THF. The solution was cooled down to 263K, thereafter *n*-butyl lithium (8 mL of 2.5M in hexanes, 20 mmol) was added dropwise. The mixture was stirred for 30 minutes, next SnCl₄ (1.3 g, 5 mmol) was added dropwise. The mixture was warmed up to the room temperature and stirred overnight. The obtained solid was recovered using vacuum filtration, washed twice with THF (200 mL), distilled water (200 mL) and ethanol (200 mL). 1.63 g of pale yellow powder were obtained.

Sn-OF-2 was synthesized following the protocol elaborated by Hausoul et al.²⁵ for the preparation of phosphorous-containing element organic frameworks. 1,3,5-Tri-(4-bromophenyl)-benzene (2.74 g, 5 mmol) was dispersed in 140 mL Et₂O. The solution was cooled down to 263 K and *n*-butyl lithium (9.375 mL of 1.6M in hexanes, 15 mmol) was added dropwise under stirring. After stirring the suspension for 30 minutes, SnCl₄ (0.98 g, 3.75 mmol) was added dropwise. The mixture was warmed up to the room temperature and stirred overnight. The obtained solid was washed with Et₂O (150 mL), THF (150 mL) distilled water (150 mL) and ethanol (150 mL). White powder (1.01 g) was obtained after drying under vacuum at room temperature.

Sn-Beta catalyst was synthesized according to Dijkmans et al.²⁶ H-Beta zeolite in a powder form was supplied by Clariant Produkte (SiO₂:Al₂O₃ = 23 mol:mol; S_{BET} = 583 m²g⁻¹). The H-Beta (10.0 g) was subjected dealumination by stirring in HNO₃ (500 mL of 7M) for 20 hours at 80 °C. After washing with of distilled water (10 L), dealuminated zeolite was dried in air and at 80°C. Prior to tin grafting, the dealuminated zeolite was kept at 150 °C in air overnight to remove adsorbed water. The material was placed in isopropanol (100 mL per g material) solution of SnCl₄ (7.73 g, 30 mmol per g material) and refluxed for 7 hours. The material was filtered, washed with isopropanol (100 mL per g), dried in air at 60 °C and calcined as follows: ramping 3 °C min⁻¹ to 200 °C, dwell for 6 hours, ramping 3 °C min⁻¹ to 550 °C, dwell for 6 hours.

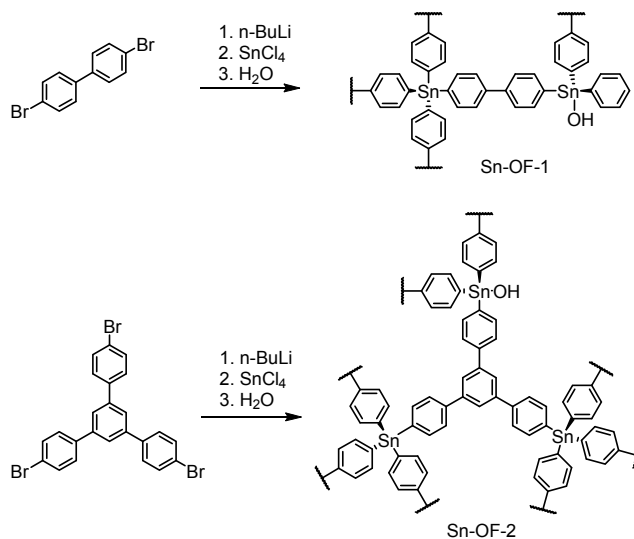
2.2. Characterization of Catalysts

The content of Sn in the materials was determined by means of inductively coupled plasma optical emission spectroscopy (ICP-OES; Spectro Analytical Instruments). Prior to the analysis Sn-Beta was dissolved in a mixture of HCl, HNO₃ and HF (5:5:1). Elemental analyses (Sn, C, H) were performed at micro analytical laboratory Kolbe (Mikrolab Kolbe), Mühlheim/Ruhr, Germany. The cata-

lysts were characterized by low-temperature sorption of N_2 using a Quadrasorb SI Automated Surface Area & Pore Size Analyzer after preliminary outgassing under vacuum at 100 °C for 20 hours. Brunauer-Emmett-Teller (BET) theory was used for calculation of the specific surface area (S_{BET}). Micropore surface areas and micropore volumes were determined using t-plot analysis. X-ray diffraction analysis (XRD) was performed on a D5000 Siemens XRD diffractometer with a $CuK\alpha$ X-Ray tube ($\lambda=1.54056 \text{ \AA}$). The tube voltage and current were 45 kV and 40 mA, respectively. Diffraction patterns were collected in the $3-90^\circ 2\theta$ range, with 0.02° intervals and a step time of 1 s. FT-IR spectra were registered using Vertex 70 (Bruker) spectrometer under diffuse reflectance mode (DRIFTS) with a dried KCl powder as a reference. The spectra were collected at room temperature in the range of 850-4000 cm^{-1} . Scanning electronic microscopy (SEM) images and energy-dispersive X-Ray (EDX) spectra were acquired using a JEOL JSM-7000F microscope (accelerating energy 15 kV) combined with EDX/EBS-System EDAX Pegasus. The samples were coated with carbon prior to SEM investigation.

2.3. Catalytic Experiments

The experiments were performed in a 20 mL autoclave equipped with a glass inlet. In a typical catalytic experiment the catalyst (100 mg) and 5 mL of 10wt.% solution of a substrate were charged in the autoclave, sealed and pressurized with 30 bar of nitrogen. The reactions were carried out under stirring at 750 rpm. After the experiments, the reaction mixture was cooled down in an ice bath and filtered through a polyamide syringe filter (pore size 0.2 μm). Commercial SnO_2 (a powder of 30-60 nm nanoparticles, 100 mg) as well as its mixture with a porous hypercrosslinked polymer prepared according to Detoni et al.²⁷ (30 mg SnO_2 and 70 mg HCP) were utilized in control experiments. The filtrates were analyzed by HPLC using a Shimadzu Prominence LC-20 system equipped with a refractive index (RI) detector. Glucose-fructose-mannose and ribose-ribulose-arabinose mixtures were separated on Accucore Amid-Hilic 0.05M trimethylamine column (Thermo Fischer, 100 mm \times 4.6 mm) at 40 °C; the eluent (90 vol.% acetonitrile + 10 vol.% 0.02 trimethylamine in water) was supplied at 1 mL min^{-1} flow rate. Xylose-xylulose-lyxose mixtures were analyzed using Aminex HPX-87P column (Bio-Rad, 300 mm \times 7.8 mm) at 80 °C using water as eluent supplied at 0.5 mL min^{-1} flow rate. The experiment with D-(^{13}C -1)glucose as substrate was performed using standard reaction conditions for 1.5 h with EtOH+ H_2O as solvent and Sn-OF-1 as catalyst. After the experiment, the solvent was evaporated under reduced pressure at 30 °C, the obtained syrup was dissolved in D_2O and analyzed by ^{13}C NMR. ^{13}C NMR spectra were recorded at Bruker AV-400 at room temperature. CH_3OH (δ 49.5 ppm) was used as internal reference for ^{13}C NMR spectra. The pH_0 was adjusted using HNO_3 with a Titroline alpha titrator unit.



Scheme 2. Synthesis of poly(arylstannanes) by an organolithium route yields 3D-crosslinked porous tin-organic frameworks with stannanol groups as catalytically active structural defects.

3. RESULTS AND DISCUSSION

The Sn-OFs were synthesized based on an organolithium route via a nucleophilic aryl lithium intermediate which is crosslinked by a tin-based precursor under formation of a Sn-C bond (Scheme 2). The product precipitates as white powder and is filtered off, washed and dried accordingly. Both Sn-OFs are X-ray amorphous and according to the nitrogen physisorption isotherms exhibit a broad pore size distribution among micro- and mesopores with specific surface areas of 350 and 506 $m^2 g^{-1}$ for Sn-OF-1 and -2, respectively (see SI). Importantly, in addition to carbon, hydrogen and tin, the presence of oxygen was detected by means of SEM-EDX (Fig. S2). Moreover, in line with the data of Wee et al.,²³ the vibrational band corresponding to Sn-OH (ν_{OH} 3640 cm^{-1})²⁸ was detected in the IR spectrum (Fig. S3). These results suggest the presence of defects in the structure of Sn-OFs, i.e., the tin-attached hydroxyl groups due to partial hydrolysis during the synthesis and work-up procedure (Scheme 2). For comparison, Sn-Beta zeolite was prepared following the protocol proposed by Dijkmans et al.²⁶

The prepared materials were first tested for the isomerization of glucose in aqueous solution (Tab. 1). The product distribution obtained in the presence of Sn-Beta is in good agreement with the literature data showing prevailing formation of fructose while mannose is obtained in lower amount.^{3, 26} In contrast to the zeolite catalyst, Sn-OFs give rise predominantly to mannose with only minor production of fructose. The same trend was observed for the temperature range of 80-120 °C, though selectivity towards mannose somewhat decreases at temperatures above 100 °C probably due to the moderate thermal stability of saccharides (Fig. 1). Owing to the hydrophobic nature of the aromatic pore walls, Sn-OFs exhibit a low wettability in pure water and initially float on top of the aqueous solution (Fig. S4). In order to improve the

Table 1. Results of catalytic experiments.

Entry	Catalyst	Substrate	Solvent	Time h	Conv. %	Ratio of monosaccharides / %			Balance %
						Aldose	Aldose Epim.	Ketose	
						Glucose	Mannose	Fructose	
1	Sn-OF-1	Glucose ^[a]	EtOH+H ₂ O	1.5	23	77	21	2	100
2	Sn-OF-1	Glucose ^[a]	H ₂ O	1.5	12	88	11	1	100
3	Sn-Beta	Glucose ^[a]	EtOH+H ₂ O	1.5	20	80	2	17	99
4	Sn-Beta	Glucose ^[a]	H ₂ O	1.5	33	68	5	27	98
5	Sn-OF-1	Mannose ^[b]	EtOH+H ₂ O	3	29	25	70	5	100
6	Sn-OF-1	Mannose ^[a]	EtOH+H ₂ O	1.5	14	11	87	2	99
7	Sn-Beta	Mannose ^[a]	EtOH+H ₂ O	1.5	37	4	63	33	100
						Arabinose	Ribose	Ribulose	
8	Sn-OF-1	Arabinose ^[b]	EtOH+H ₂ O	3	41	76	20	4	78
9	Sn-OF-1	Arabinose ^[a]	EtOH+H ₂ O	1.5	23	87	11	2	88
10	Sn-Beta	Arabinose ^[a]	EtOH+H ₂ O	1.5	49	63	19	18	82
11	Sn-OF-1	Ribose ^[b]	EtOH+H ₂ O	3	43	18	77	5	73
12	Sn-OF-1	Ribose ^[a]	EtOH+H ₂ O	1.5	39	11	86	3	71
13	Sn-Beta	Ribose ^[a]	EtOH+H ₂ O	1.5	57	22	53	25	80
						Xylose	Lyxose	Xylulose	
14	Sn-OF-1	Xylose ^[b]	EtOH+H ₂ O	3	34	74	25	1	88
15	Sn-OF-1	Xylose ^[a]	EtOH+H ₂ O	1.5	19	83	12	5	97
16	Sn-Beta	Xylose ^[a]	EtOH+H ₂ O	1.5	54	58	39	2	79
17	Sn-OF-1	Lyxose ^[b]	EtOH+H ₂ O	3	48	25	71	5	74
18	Sn-OF-1	Lyxose ^[a]	EtOH+H ₂ O	1.5	18	11	85	4	97
19	Sn-Beta	Lyxose ^[a]	EtOH+H ₂ O	1.5	21	9	88	4	90

[a] Reaction conditions: 5 mL of 10 wt.% substrate solution, 100 mg catalyst, 100 °C, 750 rpm. [b] Reaction conditions: 5 mL of 5 wt.% substrate solution, 100 mg catalyst, 100 °C, 750 rpm. The saccharide distributions at equilibrium are: glucose:mannose = 70:30; xylose:lyxose = 58:42; arabinose:ribose = 67:33.^{15, 29}

wettability of the Sn-OFs, mixtures of ethanol-water with different compositions were used as solvent. Indeed, the catalysts can be well dispersed in ethanol-water mixtures and increase of the ethanol content improves the yields of mannose (Fig. S5). The best results were obtained for a solvent mixture that contains a high content of ethanol although at concentrations above 50 wt.% the solubility of glucose decreases tremendously. Hence, a mixture of water and ethanol with a mass ratio of 1:1 was used as solvent in this study. Importantly, the product selectivity observed for Sn-OFs and Sn-Beta are independent of the solvent composition. A question of great importance is whether the catalysis with Sn-OFs is truly heterogeneous. Therefore, the filtration test, i.e., removal of the catalyst and continuation of the reaction, was carried out (Figure 1). It proved that the reaction proceeds heterogeneously since no molecular or dissolved nano-sized active species are leached into the solution. This was confirmed by elemental analysis of the liquid phase which was negative for tin. Additionally, SnO₂ as well as a physical mixture of SnO₂ with a porous, hydrophobic hypercrosslinked polymer were tested for the glucose isomerization. No conversion of the substrate was observed under the typical reac-

tion conditions (100 °C, 1.5 h). This can be explained by a low specific surface area of the used commercial SnO₂, since activity of the supported nano-SnO₂ for isomerization of glucose into fructose has been recently reported.³⁰ Though the presence of SnO₂ was not detected by XRD, formation of a SnO₂ supported amorphous phase on a Sn-OF surface cannot be excluded. These SnO₂ nanoparticles can be responsible for the formation of fructose as a by-product.

Reusability of the catalysts for the epimerization was investigated in detail (Table 2). Firstly, the used Sn-OF-1 catalyst was washed with a mixture of EtOH-H₂O and dried before recycling. In the second run the glucose conversion significantly dropped along with a dramatic decrease of the specific surface area and the pore volume of the material (Entry 1, Table 2). We hypothesized that the observed collapse of the pore structure can occur due to a contact of the material with a bulk liquid at high temperature followed by a drying. Indeed, heating a Sn-OF-1 suspension till 100 °C in a mixture of EtOH-water (without adding glucose) with a subsequent drying led to a similar textural degradation (Entry 2, Table 2). Alike

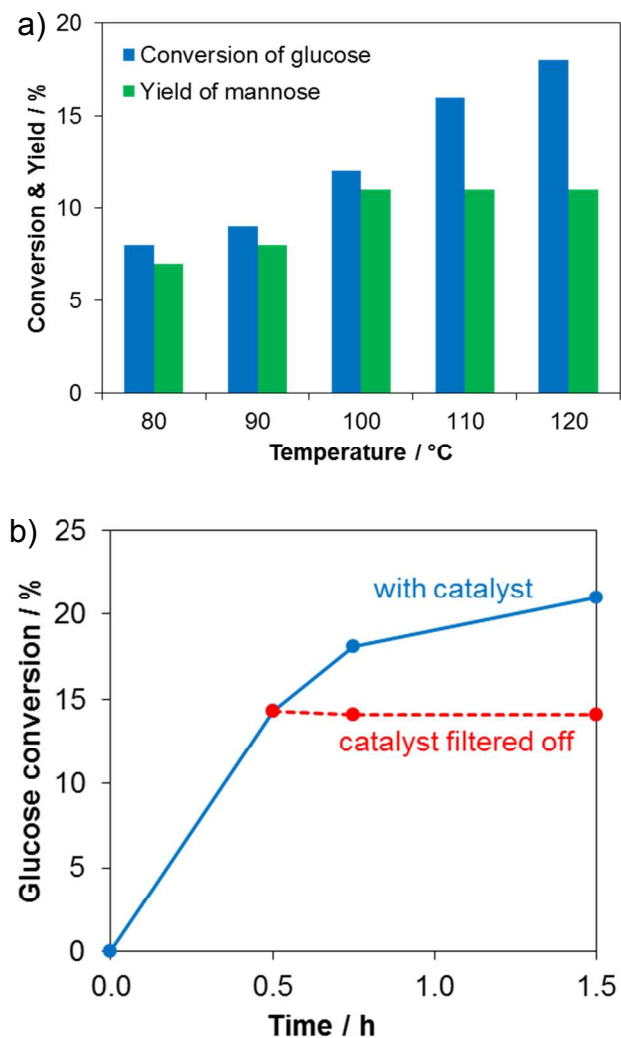


Figure 1. a) Temperature-dependent conversion of glucose and yield of mannose (reaction conditions: 5 mL of 10 wt.% substrate solution in water, 100 mg Sn-OF-1, 1.5 h, 750 rpm) and b) results of the filtration experiment to demonstrate heterogeneity of the catalyst Sn-OF-1 (reaction conditions: 5 mL of 10 wt.% substrate solution, solvent 50 vol.% H₂O + 50 vol.% EtOH, 100 mg catalyst Sn-OF-1, 100 °C, 1.5 h, 750 rpm).

breakage of pore structure was reported for silicagels or carbons due to capillary stress during the drying.³¹ Washing a material with a solvent exhibiting a low surface tension prior to drying typically improves textural properties of the dried solids. In other words, a low interfacial energy of the solvents facilitates reducing the capillary pressure and helps maintaining the high porosity.³¹ Therefore, the materials after a catalytic test were firstly rinsed with a mixture of water (surface tension 72.8 mN m⁻¹ at 20 °C) with ethanol (surface tension 22.1 mN m⁻¹ at 20 °C) to remove physically adsorbed polar molecules of saccharides. Thereafter, the catalysts were washed either with pure ethanol or with THF (surface tension 26.4 mN m⁻¹ at 20 °C) to substitute the solvent in the pores and finally dried (Entries 3, 4 and 6 in Table 2, respectively). As expected, washing with ethanol or THF results in enhancing the robustness of the material upon drying as well as improving the yield upon recycling. Additionally, the Sn-OF-1 catalyst was rinsed after the first run with an ethanol-water mixture and recycled without drying. This procedure allowed maintaining the catalytic performance in a subsequent cycle (Entry 5, Table 2). Apparently, drying procedures are to be avoided to prevent partial structural collapse of the organic framework with a loss of activity. However, elaboration of a more suitable regeneration procedure and further insight into the long-term stability of the Sn-OF-1 catalysts is required.³²⁻³³

Inspired by the excellent performance in the glucose epimerization, we performed catalytic tests for other monosaccharides (Table 1). Remarkably, the formation of the respective epimeric aldose clearly predominates in the presence of Sn-OFs for all the tested substrates. In contrast, Sn-Beta exhibits higher selectivity for the corresponding ketoses. Results of catalytic tests of Sn-OF-2 were similar to that of Sn-OF-1 (Table S3) proving that the catalytic performance is determined by the open tin-sites while the organic framework structure and the textural parameters are only of minor influence on selectivity when comparing different Sn-OFs. For a detailed understanding of the Sn-OF active sites and the differences in selectivity compared to Sn-Beta the epimerization

Table 2. Results of Sn-OF-1 recycling and its properties as fresh (left) and treated/spent (right) catalyst.

Entry	Textural properties			Results 1 st run ^[a]		Treatment ^[b]	Textural properties			Result 2 nd run	
	S _{BET} m ² g ⁻¹	S _{micro} m ² g ⁻¹	V _{pore} cm ³ g ⁻¹	C _{Glucose} %	Y _{Mannose} %		S _{BET} m ² g ⁻¹	S _{micro} m ² g ⁻¹	V _{pore} cm ³ g ⁻¹	C _{Glucose} %	Y _{Mannose} %
1	350	228	0.24	12	11	EtOH/H ₂ O; dried	38	0	0.075	5	4.6
2 ^[c]	350	228	0.24	-	-	dried	22	0	0.073	7.8	7.5
3	350	228	0.24	12	11	EtOH/H ₂ O, EtOH; dr.	70	0	0.14	8.4	8.3
4	350	228	0.24	12	11	EtOH/H ₂ O, THF; dr.	110	0	0.14	10	9
5	350	228	0.24	12	11	EtOH/H ₂ O; not dried	-	-	-	11	10
6 ^[c]	350	228	0.24	-	-	THF; dried	122	0	0.12	-	-

[a] Reaction conditions: 5 mL of 10 wt.% substrate solution, solvent 50 wt.% H₂O + 50 wt.% EtOH, 100 mg Sn-OF-1, 100 °C, 0.5 h, 750 rpm. [b] Treatment of the catalyst between the first and the second runs by washing with the respective solvent (mixture) and drying. [c] Sn-OF-1 was charged into an autoclave and heated up in 50 wt.% H₂O + 50 wt.% EtOH without glucose.

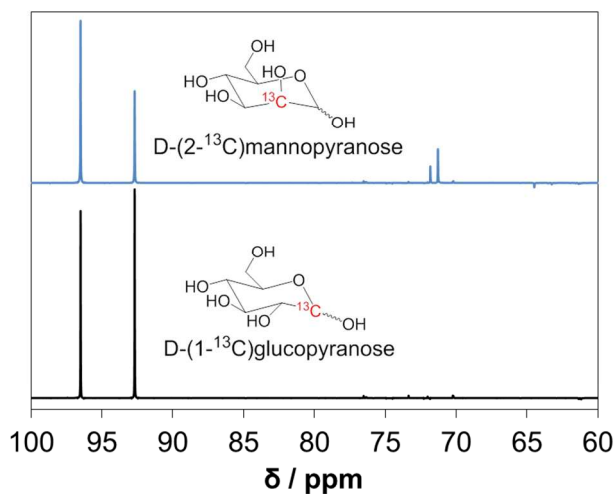


Figure 2. ^{13}C NMR spectra of D-(1- ^{13}C)glucose as a substrate (bottom) and the reaction mixture after epimerization over Sn-OF-1 (top) indicating the formation of mannose by a rearrangement of the carbon skeleton.

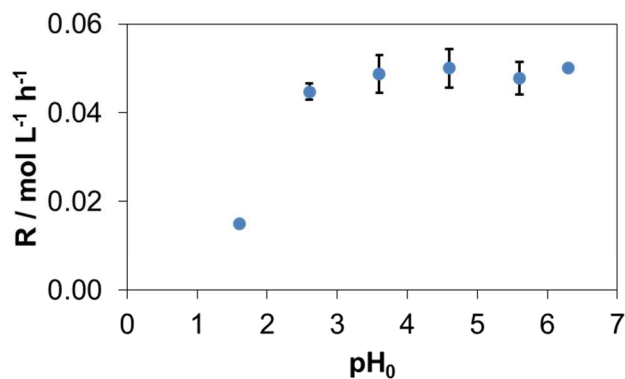
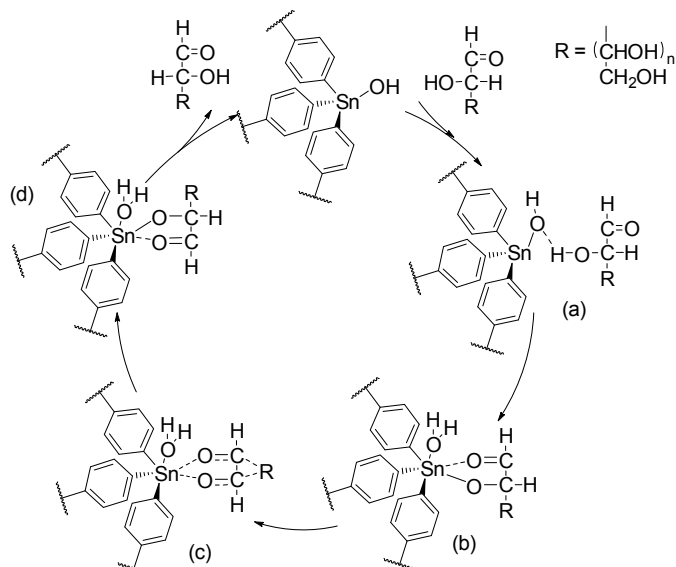


Figure 3. Dependence of the reaction rate (R) on the initial pH of the reaction mixture.

mechanism was investigated using glucose as a substrate. First, the epimerization of D-(1- ^{13}C)-glucose was studied. Analysis of the obtained product mixture by ^{13}C NMR revealed the formation of D-(2- ^{13}C)-mannose as a major product (Fig. 2). The solution of D-(1- ^{13}C)glucose demonstrated two strong resonance peaks at 96.5 and 92.5 ppm corresponding to C-1 of α -glucopyranose and β -glucopyranose, respectively.³⁴ Analyzing the reaction solution after the experiment two additional ^{13}C resonance peaks were observed at 71.3 and 71.8 ppm related to α -mannopyranose and β -mannopyranose (Fig. 2, Tab. S4).³⁴ This suggests that the reaction proceeds via rearrangement of the carbon skeleton owing to the carbon shift as depicted in Scheme 1b. Molecular model compounds of well-defined structure were investigated regarding their catalytic activity in order to gain more detailed information on the type of active sites. Especially tetraphenyltin and triphenyltin hydroxide were compared as model compounds depicting segments of an ideal crosslinked structure as well as partially hydrolyzed tin-sites, respectively (Fig. S6). Tetraphenyltin showed no



Scheme 3. Proposed reaction mechanism for the epimerization in the presence of Sn-OFs.

catalytic activity for the isomerization of glucose under the applied reaction condition. This was expected since a tetravalent tin substituted by four aromatic rings is sterically hindered and should not exhibit accessible active sites. Remarkably, mannose and fructose with 78 and 10 % selectivities were obtained when using triphenyltin hydroxide as catalyst, though the substrate conversion was lower than compared to Sn-OFs. This result highlights the catalytic significance of a hydroxyl group attached to the accessible tin-sites. Previous computational studies predicted an important role of a hydroxyl group attached to a Lewis acid site partially functioning as Brønsted base and hence, participating in activation of a substrate during the carbon shift mechanism.^{8, 13, 35} Moreover, catalytic activity of partially hydrolyzed molecular complexes $\text{M}(\text{OH})_n(\text{H}_2\text{O})_m$, where M is Al or Cr, were proven experimentally.³⁶⁻³⁸

Furthermore, investigations of the reaction rate of the epimerization revealed a significant dependence on the initial pH of the reaction mixture (Fig. 3). Increase of the hydronium ion concentration results in protonation of the hydroxyl group attached to the tin atoms and diminishes the concentration of Brønsted basic sites. Indeed, the epimerization rate decreases when increasing the acidity of the reaction medium. This proves that the OH-group bound to Sn acts as base for the activation of aldoses. Hence, the mechanism for the epimerization based on the carbon shift can be explained. For the hydride shift, numerous computational and experimental evidences also support the key role of a Lewis acidic atom and an attached hydroxyl group,^{8, 13, 35-38} which is in line with our findings. Nevertheless, the presence of a proton donor nearby the coordination sphere of a Lewis acid site is crucial for stabilization of the transition state for the hydride shift mechanism. The examples of such proton donors are an adjacent silanol for Sn-Beta¹² or bulk water for molecular salts.³⁵ Apparently, the hydrophobic linkers

of Sn-OFs disable any contacts of Sn-OH active sites with bulk water and do not bear any proton donor themselves. As a result, the absence of a proton donor next to the coordination sphere of Sn makes the Sn-OFs unique solid catalysts for the epimerization of aldoses. Hence, a reaction mechanism is proposed based on the results for the epimerization of glucose in the presence of Sn-OFs (Scheme 3). The initial step is the interaction of the Sn-OH group with the proton from the OH-group attached to C-2 (a). Under elimination of water glucose undergoes a bidentate coordination at the tin site (b). This transition state (c) enables the carbon shift of C-3 bound to C-2 towards the formation of a new C-C bond with the initial C-1 carbon. Finally, the formed epimeric aldose is desorbed and replaced again by the initial hydroxyl group resulting in a closed catalytic cycle. Based on the experimental evidence and the feasible catalytic cycle three peculiarities of Sn-OFs contribute to catalytic activation of aldoses, namely (1) Lewis acidity of Sn; (2) Brønsted basicity of the hydroxyl groups attached to Sn and (3) highly hydrophobic environment of the Sn-OH active sites due to aromatic organic linkers.

4. CONCLUSION

In conclusion, it is shown that porous tin-organic frameworks are versatile materials that especially outstand due to accessible Sn-sites as catalytically active centers. The Sn-OFs differ from conventional solid Sn-based catalysts such as the zeolite Sn-Beta by the organic backbone resulting in highly hydrophobic confined pore spaces and isolated as well as partially hydrolyzed Sn-sites. Due to this characteristic, Sn-OFs show a unique catalytic behavior as first solid catalysts able to epimerize aldose sugars in aqueous solutions with an outstanding selectivity. The materials exhibit no leaching of Sn-species as proven by filtration experiments, thus, demonstrating their heterogeneous character. Based on isotope exchange experiments with ^{13}C -labeled substrates the mechanisms via the carbon shift route is proven and a feasible catalytic cycle is proposed. Overall, this work demonstrates the potential of porous organic frameworks in applications that require defined active sites. Furthermore, the applicability for selective heterogeneous catalysis in the aqueous phase is proven, thus, tackling one of the major challenges in the development of tailored biorefinery schemes to selectively convert biogenic platform chemicals.

AUTHOR INFORMATION

Corresponding Author

* Dr. Marcus Rose (rose@itmc.rwth-aachen.de)

Notes

The authors declare no competing financial interest.

ASSOCIATED CONTENT

Supporting Information

N_2 physisorption isotherms, textural properties, elemental analysis, SEM-EDX, DRIFTS, additional data of catalytic

experiments, ^{13}C NMR chemical shifts of isotope labeled sugars. This material is available free of charge via the Internet at <http://pubs.acs.org>.

ACKNOWLEDGMENT

We gratefully acknowledge financial support by the German Research Foundation (Deutsche Forschungsgemeinschaft, DFG, RO 4757/5-1) and the excellence initiative. ID thanks the Alexander von Humboldt Foundation and the Bayer Foundation for the financial support. We also thank Noah Avraham for the HPLC quantification, Heike Bergstein for ICP OES analysis, and Karl-Josef Vaessen for TG and XRD measurements. Regina Palkovits is gratefully acknowledged for valuable discussions and the opportunity to carry out independent research in her group.

REFERENCES

- (1) Lichtenthaler, F. W., The Key Sugars of Biomass: Availability, Present Non-Food Uses and Potential Future Development Lines. In *Biorefineries - Industrial Processes and Products. Status Quo and Future Directions*, Kamm, B.; Gruber, P. R.; Kamm, M., Eds. Wiley-VCH Verlag: Weinheim, 2006; Vol. 2, pp. 3-59.
- (2) Bozell, J. J.; Petersen, G. R., *Green Chem.* **2010**, *12*, 539-554.
- (3) Delidovich, I.; Palkovits, R., *ChemSusChem* **2016**, *9*, 547-561.
- (4) Moliner, M.; Román-Leshkov, Y.; Davis, M. E., *Proc. Natl. Acad. Sci. U.S.A.* **2010**, *107*, 6164-6168.
- (5) Gounder, R.; Davis, M. E., *AIChE J.* **2013**, *59*, 3349-3358.
- (6) Gounder, R.; Davis, M. E., *J. Catal.* **2013**, *308*, 176-188.
- (7) Osmundsen, C. M.; Holm, M. S.; Dahl, S.; Taarning, E., *Proc. R. Soc. A* **2012**, *468*, 2000-2016.
- (8) Bermejo-Deval, R.; Assary, R. S.; Nikolla, E.; Moliner, M.; Román-Leshkov, Y.; Hwang, S.-J.; Palsdottir, A.; Silverman, D.; Lobo, R. F.; Curtiss, L. A.; Davis, M. E., *Proc. Natl. Acad. Sci. U.S.A.* **2012**, *109*, 9727-9732.
- (9) Bermejo-Deval, R.; Orazov, M.; Gounder, R.; Hwang, S.-J.; Davis, M. E., *ACS Catal.* **2014**, *4*, 2288-2297.
- (10) Christianson, J. R.; Caratzoulas, S.; Vlachos, D. G., *ACS Catal.* **2015**, *5*, 5256-5263.
- (11) Román-Leshkov, Y.; Moliner, M.; Labinger, J. A.; Davis, M. E., *Angew. Chem. Int. Ed.* **2010**, *49*, 8954-8957.
- (12) Rai, N.; Caratzoulas, S.; Vlachos, D. G., *ACS Catal.* **2013**, *3*, 2294-2298.
- (13) Li, G.; Pidko, E. A.; Hensen, E. J. M., *Catal. Sci. Technol.* **2014**, *4*, 2241-2250.
- (14) Bilik, V., *Chem. Zvesti* **1972**, *26*, 183-186.
- (15) Petruš, L.; Petrušová, M.; Hricoviniová, Z., The Bilik Reaction. In *Glycoscience*, Springer Berlin / Heidelberg: 2001; Vol. 215, pp 15-41.
- (16) Brand, S. K.; Labinger, J. A.; Davis, M. E., *ChemCatChem* **2016**, *8*, 121-124.
- (17) Brand, S. K.; Josephson, T. R.; Labinger, J. A.; Caratzoulas, S.; Vlachos, D. G.; Davis, M. E., *J. Catal.* **2016**, *341*, 62-71.
- (18) Gunther, W. R.; Wang, Y.; Ji, Y.; Michaelis, V. K.; Hunt, S. T.; Griffin, R. G.; Román-Leshkov, Y., *Nat. Commun.* **2012**, *3*, 1109.
- (19) Dobler, W.; Ernst, H.; Paust, J., *US Patent US 4778531 A* **1988**.
- (20) Takagaki, A.; Furusato, S.; Kikuchi, R.; Oyama, S. T., *ChemSusChem* **2015**, *8*, 3769-3772.
- (21) Köckritz, A.; Kant, M.; Walter, M.; Martin, A., *Appl. Catal. A Gen.* **2008**, *334*, 112-118.
- (22) Samuel, J.; Tanner, M. E., *Nat. Prod. Rep.* **2002**, *19*, 261-277.
- (23) Fritsch, J.; Rose, M.; Wollmann, P.; Böhlmann, W.; Kaskel, S., *Materials* **2010**, *3*, 2447-2462.
- (24) Wee, L.; Lescouet, T.; Fritsch, J.; Bonino, F.; Rose, M.; Sui, Z.; Garrier, E.; Packet, D.; Bordiga, S.; Kaskel, S.; Herskowitiz, M.; Farrusseng, D.; Martens, J., *Catal. Lett.* **2013**, *143*, 356-363.
- (25) Hausoul, P. J. C.; Eggenhuisen, T. M.; Nand, D.; Baldus, M.; Weckhuysen, B. M.; Klein Gebbink, R. J. M.; Bruijninx, P. C. A., *Catal. Sci. Technol.* **2013**, *3*, 2571-2579.
- (26) Dijkmans, J.; Gabriels, D.; Dusselier, M.; de Clippel, F.; Vanelderden, P.; Houthoofd, K.; Malfliet, A.; Pontikes, Y.; Sels, B. F., *Green Chem.* **2013**, *15*, 2777-2785.

- 1
2
3
4
5
6
7
8
9
10
11
12
13
14
15
16
17
18
19
20
21
22
23
24
25
26
27
28
29
30
31
32
33
34
35
36
37
38
39
40
41
42
43
44
45
46
47
48
49
50
51
52
53
54
55
56
57
58
59
60
- (27) Detoni, C.; Gierlich, C. H.; Rose, M.; Palkovits, R., *ACS Sustainable Chem. Eng.* **2014**, *2*, 2407-2415.
(28) Amalric-Popescu, D.; Bozon-Verduraz, F., *Catal. Today* **2001**, *70*, 139-154.
(29) Angyal, S. J., *Angew. Chem. Int. Ed.* **1969**, *8*, 157-166.
(30) Bermejo-Deval, R.; Gounder, R.; Davis, M. E., *ACS Catal.* **2012**, *2*, 2705-2713.
(31) Brinker, C. J.; Scherer, G. W., *Sol-Gel Science. The Physics and Chemistry of Sol-Gel Processing*. Academic Press: San Diego, 1990; p 908.
(32) Delidovich, I.; Palkovits, R., *Catal. Sci. Technol.* **2014**, *4*, 4322-4329.
(33) Lari, G. M.; Dapsens, P.-Y.; Scholz, D.; Mitchell, S.; Mondelli, C.; Perez-Ramirez, J., *Green Chem.* **2016**, *18*, 1249-1260.
(34) King-Morris, M. J.; Serianni, A. S., *J. Am. Chem. Soc.* **1987**, *109*, 3501-3508.
(35) Mushrif, S. H.; Varghese, J. J.; Vlachos, D. G., *Phys. Chem. Chem. Phys.* **2014**, *16*, 19564-19572.
(36) Tang, J.; Guo, X.; Zhu, L.; Hu, C., *ACS Catal.* **2015**, *5*, 5097-5103.
(37) Choudhary, V.; Pinar, A. B.; Lobo, R. F.; Vlachos, D. G.; Sandler, S. I., *ChemSusChem* **2013**, *6*, 2369-2376.
(38) Choudhary, V.; Mushrif, S. H.; Ho, C.; Anderko, A.; Nikolakis, V.; Marinkovic, N. S.; Frenkel, A. I.; Sandler, S. I.; Vlachos, D. G., *J. Am. Chem. Soc.* **2013**, *135*, 3997-4006.

1 SYNOPSIS TOC (Word Style "SN_Synopsis_TOC").
2
3

4 Porous tin-organic frameworks as solid catalysts enable a heterogeneously catalyzed epimerization of sugars in
5 aqueous solutions. The hydrophobic pores in combination with accessible and partially hydrolyzed tin sites are
6 responsible for an outstanding selectivity. This example demonstrates the potential of novel hybrid materials especially
7 in the field of catalysis for tailor-made biogenic platform chemicals.
8
9

10
11 For Table of Contents (TOC) only
12

